www.sciencemag.org/cgi/content/full/science.1204592/DC1

Supporting Online Material for

TFEB Links Autophagy to Lysosomal Biogenesis

Carmine Settembre, Chiara Di Malta, Vinicia Assunta Polito, Moises Garcia Arencibia, Francesco Vetrini, Serkan Erdin, Serpil Uckac Erdin, Tuong Huynh, Diego Medina, Pasqualina Colella, Marco Sardiello, David C. Rubinsztein, Andrea Ballabio*

*To whom correspondence should be addressed. E-mail: ballabio@tigem.it

Published 26 May 2011 on *Science* Express
DOI: 10.1126/science.1204592

This PDF file includes

Materials and Methods ("TFEB links Autophagy to Lysosomal Biogenesis" by Settembre et al.)

Cell culture and media and drugs treatment

HeLa and COS cells were purchased from ATCC. Mouse embryonic fibroblasts (MEF) were obtained from E14.5 embryos. Cells were cultured in the following media: (normal) DMEM high glucose supplemented with 10% FBS; (starvation) HBSS media with Ca and Mg supplemented with 10mM HEPES; (Serum) EBSS supplemented with 20%FBS; (amino acid media) Glucose and serum free DMEM;

Drugs treatment: Rapamycin (0.25mg/ml, SIGMA) 4h otherwise indicated; Bafilomycin, (400nM, SIGMA) for the indicated time; Insulin (100ng/ml SIGMA) for 2h; EGF, FGF (BD biosciences); LIF (100ng/ml; esgro-millipore) 2h; PMA (1μg/ml) 2h. To inhibit MAPK we used: U0126 25mM (Cell Signaling)+ SB203580 20μM+ JNK inhibithor II 10μM (Calbiochem). API2 (AKT inhibitor) were used at 1μM. Lysosomal inhibitors were pepstatin and E64 (10mg/ml 4h SIGMA).

Transfection and siRNA

Both plasmids and siRNA were transfected with lipofectamine LTX (Invitrogen) using a reverse transfection protocols. For RNA analysis cells were collected 24h after transfection, for protein analysis 48h otherwise indicated. SiRNA-transfected cells were collected after 48 or 72h. siRNA TFEB were used at 50nM (Dharmacon), siRNA ERK1/2 were used at 100nM (Cell Signaling).

Western blotting

Cells were solubilized in RIPA buffer supplemented with protease and Phosphatase inhibitors (SIGMA). Tissues were solubilized in RIPA supplemented with 1%SDS and briefliy sonicated. From 10 to 30 micrograms were loaded on 4-12% Bis-Tris gel (NUPAGE, Invitrogen), transferred to PVDF membranes and analyzed by western blot using the ECL method (Pierce). The following antibodies were used: LC3 (Novus Biological), FLAG, b-ACTIN, TUBULIN (SIGMA), HA (Covance), H3, ERK1/2, p-

ERK1/2, p-AKT, p-70S6K (Cell Signaling), ERK2 (Santa Cruz). Protein levels were quantified by using ImageJ software analysis.

Nuclear/cytosolic fractionation

Cells at 50% of confluence in 6 well dishes were serum starved overnight (ON). In the morning starving media (supplemented with kinase inhibitor where indicated) was added at least for 1h to achieve complete starvation. Subsequently, indicated media was added for at least 1h prior to harvest. Subcellular fractionation was carried out as follows: Briefly, cells were lysed in 0.5 Triton X-100 lysis buffer (50mM Tris-HCl, 0.5% triton, 137.5 mM NaCl, 10% glycerol, 5 mM EDTA supplemented with fresh protease and phosphatase inhibitors. After 15 minutes the lysate was centrifugated. The supernatant represented cytosolic fraction while pellet (nuclear fraction) was washed twice and lysed in 0.5 Triton X-100 buffer 0.5% SDS and sonicated.

Degradation of long-lived proteins

Sub-confluent cells were incubated with L-U^{14}C-serine for 20h and chased for 1h with cold media to degrade short-lived proteins. Subsequently cells were incubated with either normal media or starvation media (eventually in the presence of 3-MA) for 4h. The rate of long-lived protein degradation was calculated from the ratio of soluble radioactivity in the media to that insoluble in the acid-precipitable cell pellet.

RNA extraction, reverse transcription, ChIP and quantitative PCR

Total RNA was extracted from tissues using TRIzol (Invitrogen) or from cells using RNAesy column (Qiagen). Reverse transcription was performed using TaqMan reverse transcription reagents (Applied Biosystems). Lysosomal gene specific primers were previously reported (6). Autophagy gene primers and mouse primers were purchased from SABiosciences. Fold change calculations were calculated using SABiosciences' online data analysis website (http://www.sabiosciences.com/pcr/arrayanalysis.php) which uses the DDC_t method. In brief, the average of the most stable housekeeping genes (GAPDH, ACTB, B2M, RPL13A and HPRT) were used as "normalizer" genes to calculate the DC_t value. Next, the DDC_t value is calculated between the "control" group

and the "experimental" group. Lastly, the fold change is calculated using $2^{(-DDCt)}$. Biological replicates were grouped to allow calculating the fold change.

Protein kinase prediction

We used five methods including CrPhos0.8 (11), GPS-2.1 (12), PhosphoMotifFinder (13), Networkin (14) and PHOSIDA (15) using the default parameters. We further filtered CrPhos0.8 and GPS-2.1 predictions according to their confidence scores. For the former, we took into account the predictions with a false positive rate (FPR) equals or less than 30%. For the latter, we considered the predictions with score equals or higher than 5. GPS-2.1 scores were calculated as the difference between actual score and threshold values. We took all the predictions from other three methods. In the case of Networkin, we combined predictions from both Networkin and Networkin 2. Each method describes the kinases associated by S142 site in a different kinase classification, which simply involves four hierarchical levels: kinase group, kinase family, kinase subfamily and kinase itself. To obtain a general consensus in each hierarchical level, we classified each prediction in these four hierarchical levels, if the predictions were not already classified in that manner. We searched for the missing classifications at the http://kinase.org/kinbase database under vertebrate clade and human species. Consensus in each classification is found according to the majority vote in each classification.

In vitro kinase assay

TFEB-S-142 (PPPAASPGVRAGHVLSSSAGNSAPNSPMAMLHIGSNPERELDDV IDNIMR) and TFEB-A-142 (PPPAASPGVRAGHVLSSSAGNSAPNAPMAM LHIGSNPERELDDVIDNIMR) were synthesized by GENESCRIPT corp. The test peptides TFEB-A-142 and TFEB-S-142 were made up to 1 mM in 50 mM HEPES pH7. There appeared to be no issue with dissolution. The kinase assay was performed at room temperature for 40 minutes at 200 μM ATP and 100 μM of each peptide, using Millipore's standard radiometric assay. All protein kinases were used at their standard KinaseProfiler™ assay concentration. Following incubation, all assays were stopped by the addition of acid and an aliquot spotted onto P30 and Filtermat A to separate products.

All tests were carried out in triplicate, and the usual substrate for each protein kinase included as a control.

In vivo gene delivery

Mice were housed in the transgenic mouse facility of Baylor College of Medicine (Houston, TX, USA). GFP-LC3 transgenic mice were a kind gift of N. Mizushima. C57B6 female mice (6-8 weeks old) were also used. The AAV vector was produced by the TIGEM AAV Vector Core Facility. Briefly, the mouse TFEB (TcFEB) coding sequence was cloned into the pAAV2.1-CMV-GFP plasmid by replacing the GFP sequence and fused in frame with a HA tag. The resulting pAAV2.1-CMV-TcFEB-HA was then triple transfected in sub-confluent 293 cells along with the pAd-Helper and the pack2/9 packaging plasmids. The recombinant AAV2/9 vectors were purified by two rounds of CsCl. Vector titers, expressed as genome copies (GC/mL), were assessed by both PCR quantification using TaqMan (Perkin-Elmer, Life and Analytical Sciences, Waltham, MA) and by dot blot analysis. Each mouse was retro-orbital injected with 1.25 $x10^{11}$ viral particle and sacrificed after 3 weeks. Starved mice were food-deprived for 16h when analyzed for gene expression, or for 24h when analyzed for GFP-LC3 dots number.

Histology and immunofluorescence

Liver samples were collected and fixed overnight in 4% paraformaldehyde in PBS. After cryoprotection in 30% sucrose in PBS, the specimens were frozen in OCT (Sakura Finetech, Torrance, CA) and sectioned 30μm thick. Images were taken on an Axioplan2 (Zeiss, Thorwood, NY). For immunofluorescence, slices were blocked for 2h at RT in 2.5% BSA in PBS+0.1% Triton X-100. After blocking, specimens were incubated for 20h with the primary antibody and, after 3X washes in PBS+0.05% TX-100, for 3h with secondary antibodies conjugated either with Alexafluor 488 or Alexafluor 555 (Invitrogen). For immunohistochemistry analyses of HA the avidin-biotin complex (ABC) method was used (Vectastain Elite ABC kit).

Electron microscopy

Control and TFEB-overexpressing cells were washed with PBS, and fixed in 1% glutaraldehyde dissolved in 0.2 M Hepes buffer (pH 7.4) for 30 min at room temperature. The cells were then postfixed for 2 h in OsO4. After dehydration in graded series of ethanol, the cells were embedded in Epon 812 (Fluka) and polymerized at 60°C for 72 h. Thin sections were cut at the Leica EM UC6, counterstained with uranyl acetate and lead citrate. EM images were acquired from thin sections using a Philips Tecnai-12 electron microscope equipped with an ULTRA VIEW CCD digital camera (Philips, Eindhoven, The Netherlands). Quantification of vacuolization was performed using the AnalySIS software (Soft Imaging Systems GmbH, Munster, Germany). Selection of cells for quantification was based on their suitability for stereologic analysis, i.e. only cells sectioned through their central region (detected on the basis of the presence of Golgi membranes) were analyzed.

Animal models

All procedures involving mice were approved by the Institutional Animal Care and Use Committee of the Baylor College of Medicine. GFP-LC3 transgenic line was described previously. Tissue specific overexpression of Tcfeb was generated as follows: *Tcfeb*-3xFlag cDNA was inserted after a CAGCAT cassette [chicken actin promoter (CAG) followed by chloramphenicol acetyltransferase (CAT) cDNA flanked by 2 loxP sites] and used to generate transgenic mice (Baylor College of Medicine transgenic core). Mice were then crossed with Albumin-CRE (obtaine from the Jackson laboratory) line.

6. M. Sardiello *et al.*, A gene network regulating lysosomal biogenesis and function. *Science* **325**, 473 (Jul 24, 2009).
11. T. H. Dang, K. Van Leemput, A. Verschoren, K. Laukens, Prediction of kinase-specific phosphorylation sites using conditional random fields. *Bioinformatics* **24**, 2857 (Dec 15, 2008).
12. Y. Xue *et al.*, GPS 2.0, a tool to predict kinase-specific phosphorylation sites in hierarchy. *Mol Cell Proteomics* **7**, 1598 (Sep, 2008).
13. R. Amanchy *et al.*, A curated compendium of phosphorylation motifs. *Nat Biotechnol* **25**, 285 (Mar, 2007).
14. R. Linding *et al.*, Systematic discovery of in vivo phosphorylation networks. *Cell* **129**, 1415 (Jun 29, 2007).

15. F. Gnad *et al.*, PHOSIDA (phosphorylation site database): management, structural and evolutionary investigation, and prediction of phosphosites. *Genome Biol* **8**, R250 (2007).

Supplementary Fig. 1

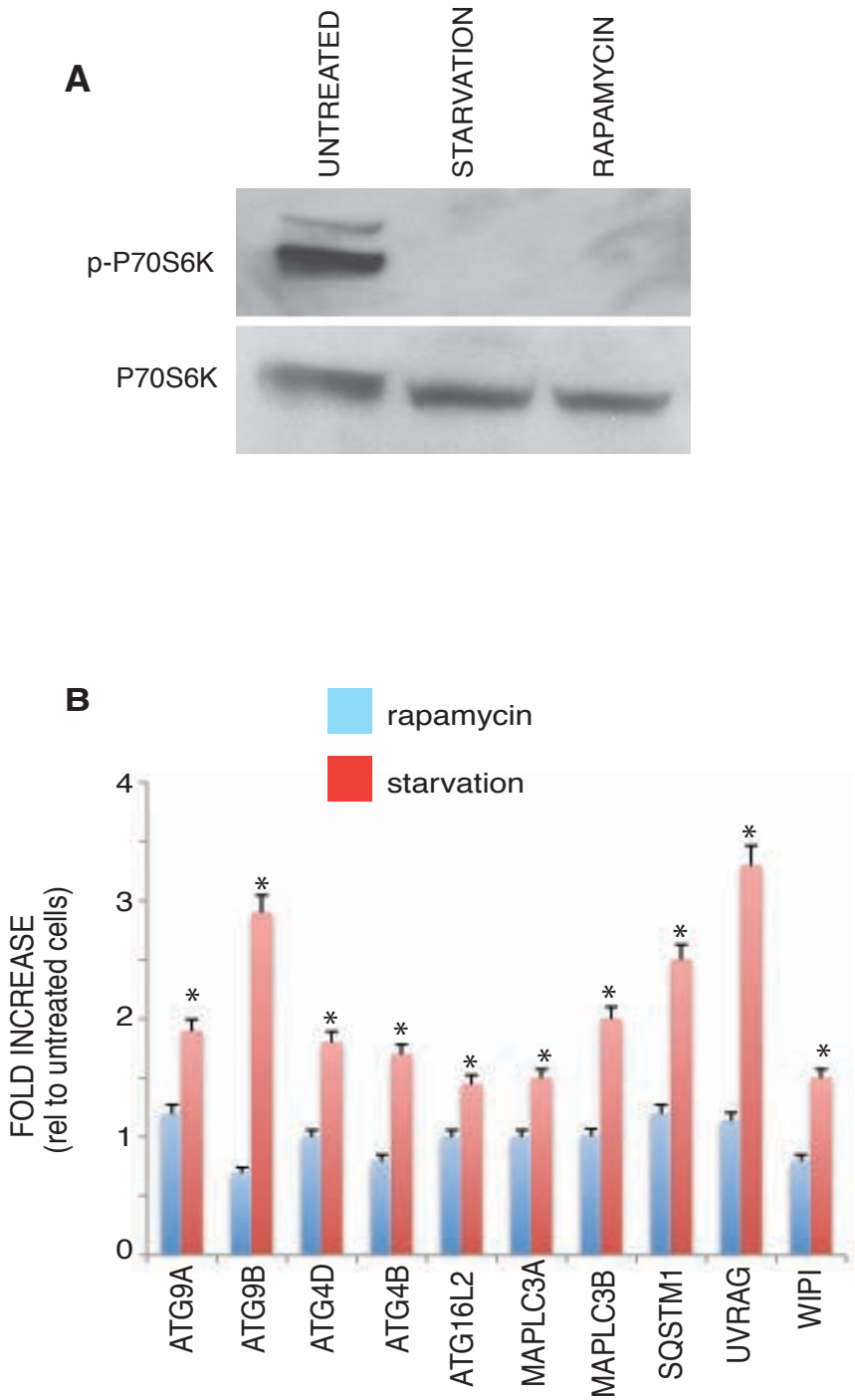

Supplementary Fig. 1 Nutrient starvation up-regulates the expression of several autophagy-related genes independently of mTORC1. (A) Starvation and rapamycin inhibit mTORC1 activity. HeLa cells were cultured in HBSS or treated with 0.25 mg/ml of Rapamycin for 4h. 30 µg of protein extract were analyzed for p-P70S6K immunoreactivity. P70S6K was used as loading control. (B) The expression level of several autophagy genes was analyzed by qPCR in HeLa cells starved or treated with rapamycin. Values are expressed as fold increase compared to untreated cells. Error bars represent standard deviation of 3 independent experiments. T-Test (unpaired); p value (*)<0.05.

Supplementary Fig. 2

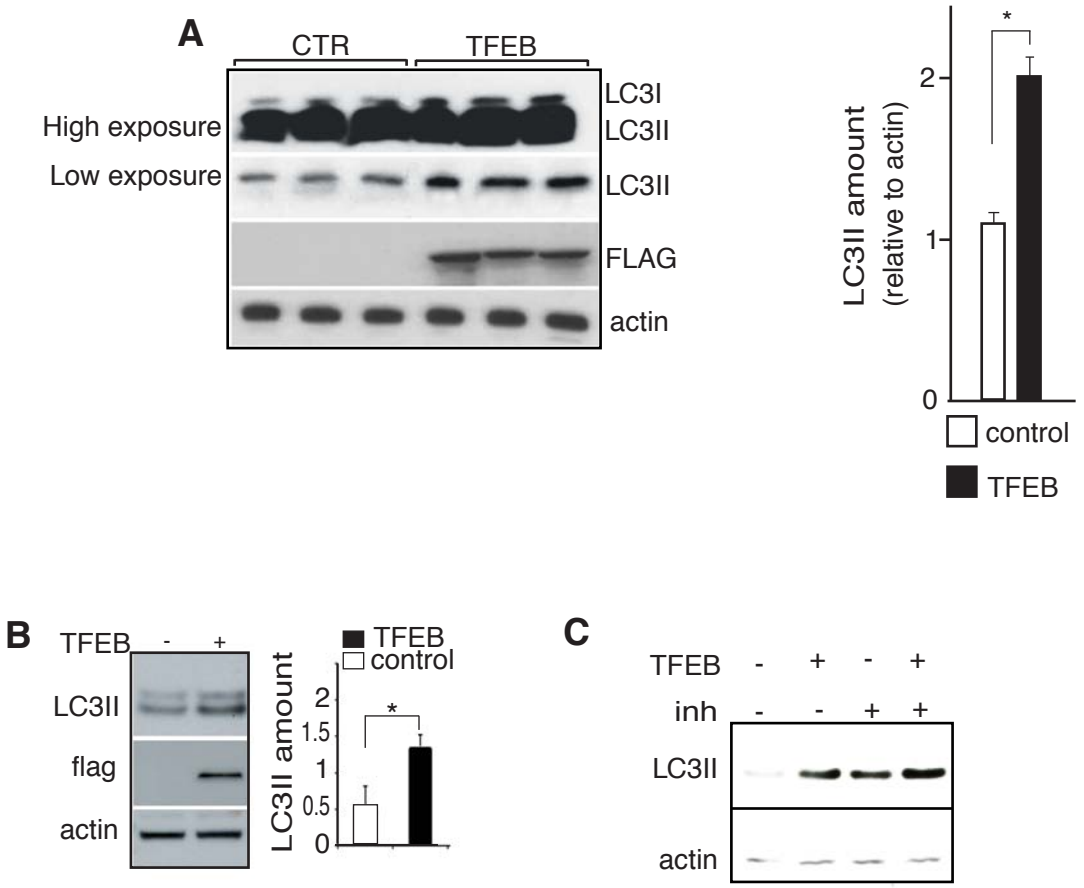

Supplementary Fig. 2 TFEB transient overexpression induces autophagy. (A) HeLa cells were transiently transfected with a plasmid encoding for flagged TFEB protein. 48h after transfection cells were collected, lysed and 10 μg of protein samples were analyzed for LC3, Flag and actin immunoreactivity. (B) Western blot analysis of LC3 in TFEB-3xflag stable overexpressing (+) and control cells (-). (C) COS-7 cells were transiently transfected with an empty vector or with a TFEB-3xFlag vector. 24h later cells were treated for 4h with lysosomal inhibitors (pepstatin/E64, 10μg/ml, SIGMA). 10 μg of cell lysates were subjected to LC3 and actin immunoblotting. Experiments were performed in triplicate and band intensities were quantified using image j software analysis. Error bars represent standard deviations; p value (*)<0.05.

Supplementary Fig. 3

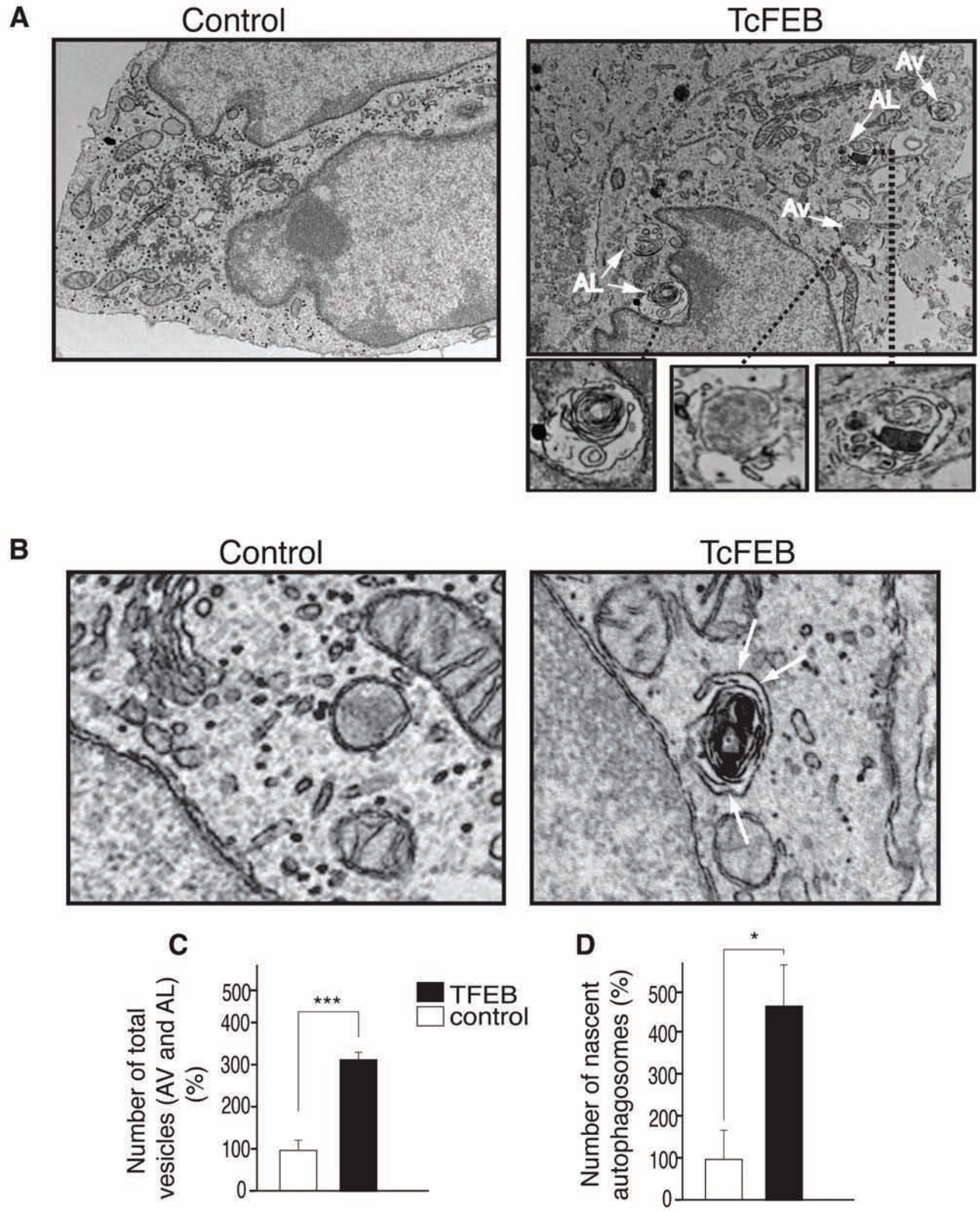

Supplementary Fig. 3 Induction of autophagy in TcFEB overexpressing MEFs. (A,B) Electron micrograph of MEFs infected with lentivirus expressing TcFEB and control cells. (A) Autophagic structures were observed upon TcFEB expression, including autophagosomes (AV) (filled with undigested cytoplasmatic material) and autolysosomes (AL) (filled with partially degraded content). (B) Formation of nascent autophagosomes was identified as a double isolation membrane (arrows) surrounding electron-dense cytoplasmatic material. (C) Quantification of number of autophagic structures (AV and AL) and (D) of nascent autophagosomes. At least 30 cells/group were analyzed. Error bars represent SEM; p value (*) < 0.05; (***)< 0.0001.

Supplementary Fig. 4

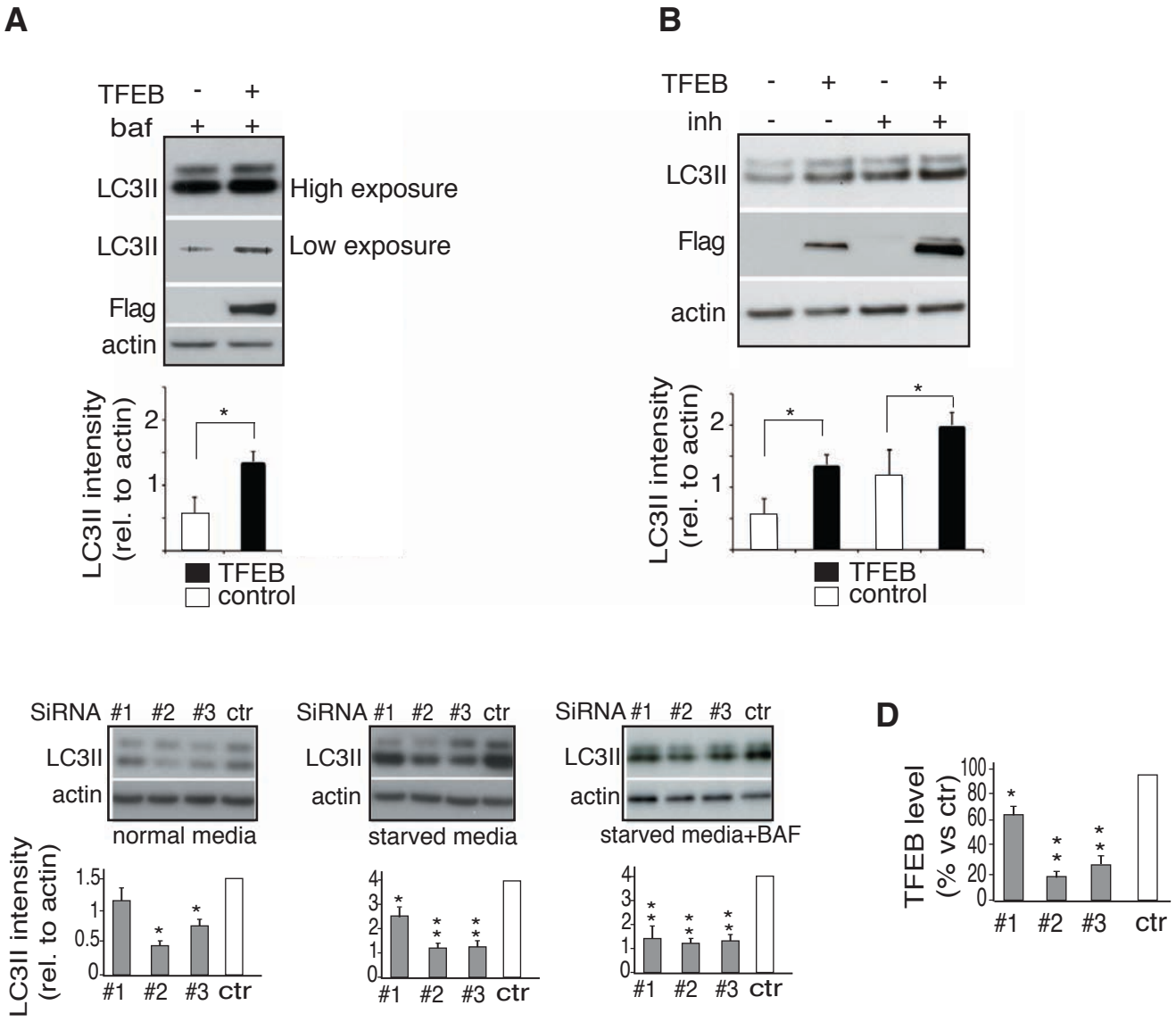

Supplementary Fig. 4 TFEB promotes autophagosome formation. (A) Control and stable TFEB-overexpressing cells were treated with bafilomycin (baf; 12h 400nM) harvested and subjected to LC3II, Flag and actin immunoblotting. (B) Control and TFEB-overexpressing cells were left untreated or treated with 10µg/ml lysosomal inhibitor pepstatin/E64 for 4h, lysed and subjected to LC3, Flag and actin immunoblotting. (C) Cellular lysates isolated from TFEB-RNAi and control cells treated with scrambled RNAi (ctr) cultured in normal media (right), starved media (center), or starved media supplemented with bafilomycin (4h; 400nM) (right). Graphs represent the quantification of LC3II expression (relative to actin) from three independent blots. (D) TFEB mRNA levels were analyzed by qPCR using cDNAs prepared from cells transfected with 3 different siRNA oligos targeting TFEB (oligo #1, #2, #3), or with a scrambled siRNA oligo (ctr). Experiments were performed in triplicate and band intensities were quantified using image j software analysis. Error bars represent standard deviations; p value (*)<0.05; (**)<0.01.

Supplementary Fig. 5

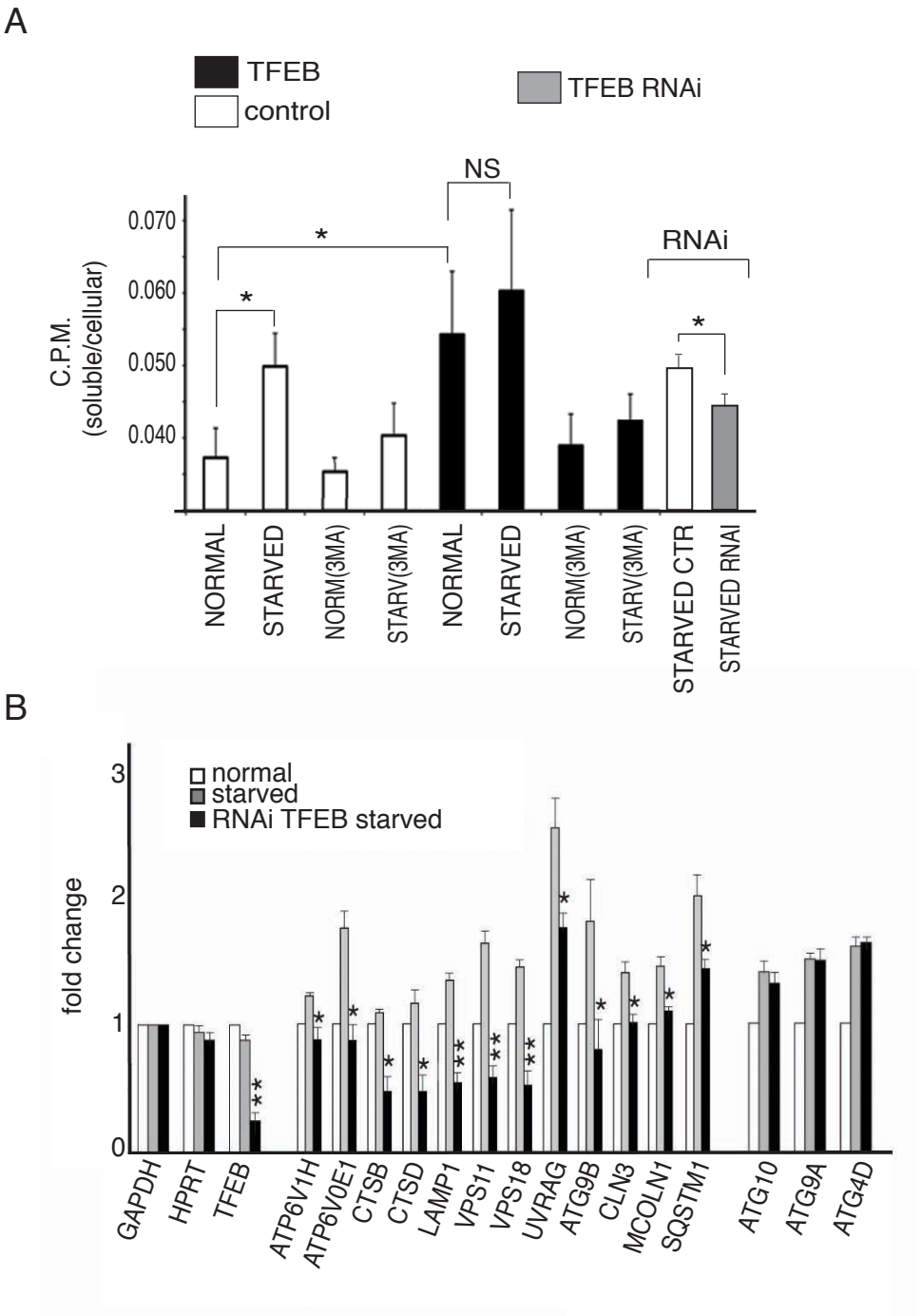

Supplementay Fig. 5 TFEB increases autophagic proteolysis. (A) Rate of long-lived protein degradation in TFEB-overexpressing, TFEB-depleted and control cells in either normal or starved conditions. 3-methyl adenine (3MA) was added where indicated. (B) qPCR analysis of TFEB-target gene expression in normal, starved, and in TFEB-siRNA starved cells. GAPDH and HPRT represent housekeeping genes, while ATG10, ATG9A and ATG4D represent control genes (non-TFEB target genes). Error bars represent standard deviations. p value (*)<0.05; (**)<0.01

Supplementary Fig. 6

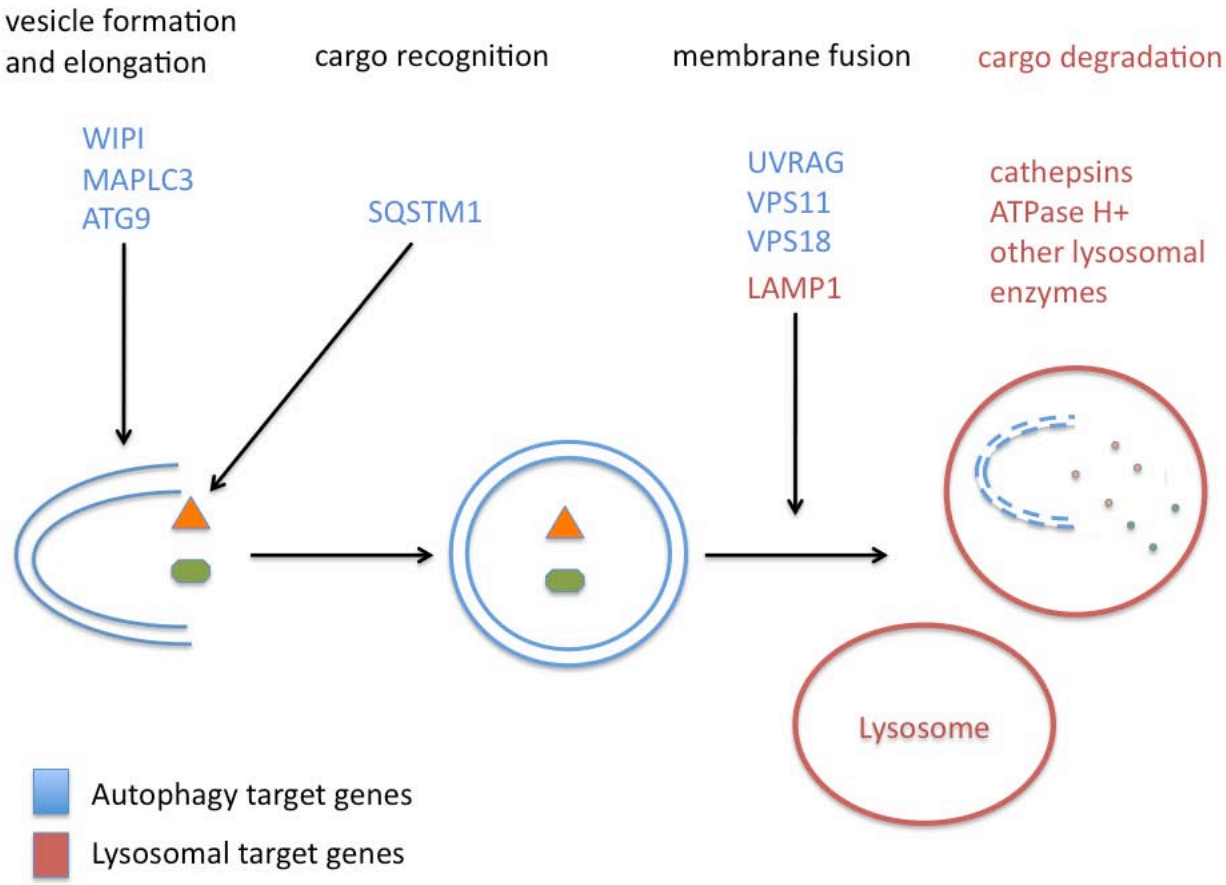

Supplementary Fig. 6 Schematic representation of the role of TFEB target genes in sequential steps of autophagy.

Supplementary Fig. 7

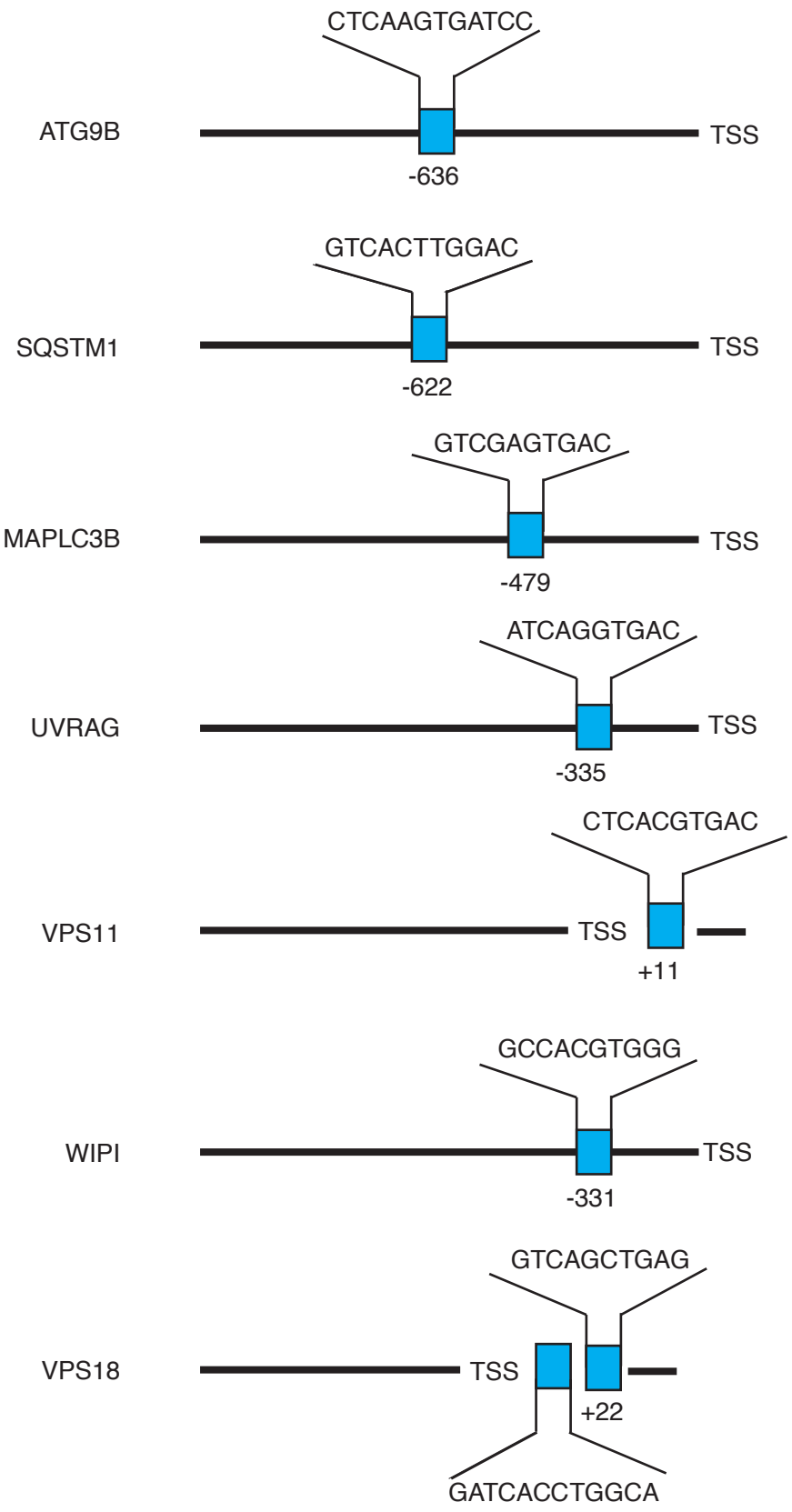

Supplementary Fig. 7 Distribution of the TFEB putative binding elements in the promoter regions of a subset of autophagy genes. Numbers indicate the distance of the binding element from the transcription start site (TSS).

Supplementary Fig. 8

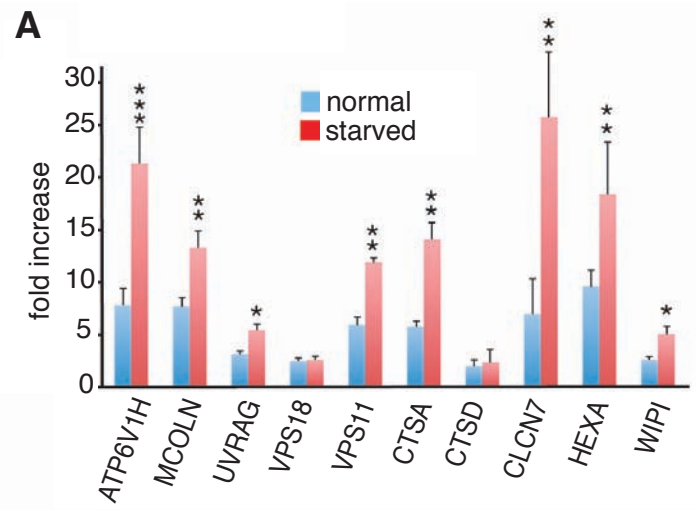

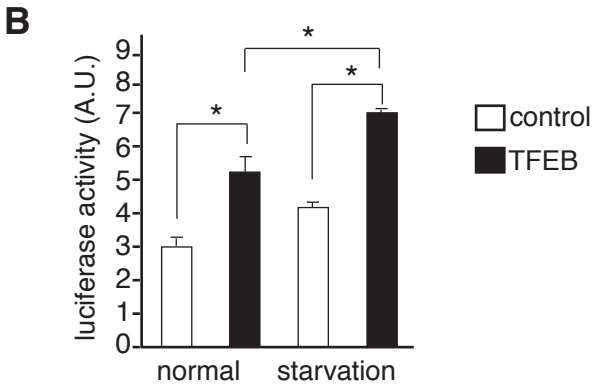

Supplementary Fig. 8 Starvation enhances TFEB activity. (A) Chromatin immunoprecipitation (ChIP) analysis. The histogram shows the amount of immunoprecipitated DNA as detected by qPCR assay. Values were normalized to the input and plotted as relative enrichment over a mock control. (B) Luciferase report assay using a construct carrying four tandem copies of TFEB binding sites. Both normal and TFEB-overexpressing HeLa cells were transfected with an artificial promoter with TFEB binding sites. Both cell types displayed an increased transactivation potential when cultured in starved conditions. Experiments were performed in triplicate. Error bars represent standard deviations; p value (*)<0.05; (**)<0.01.

Supplementary Fig. 9

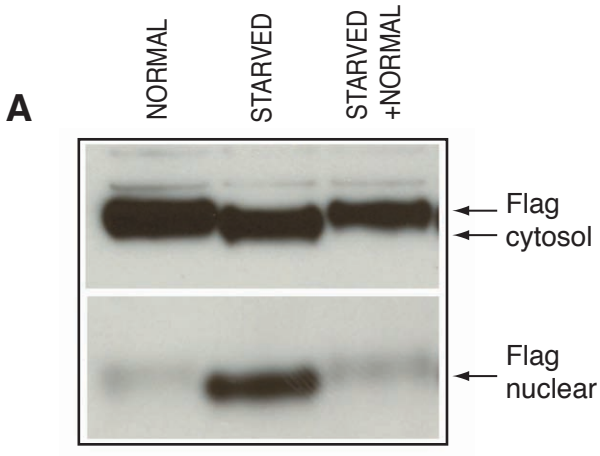

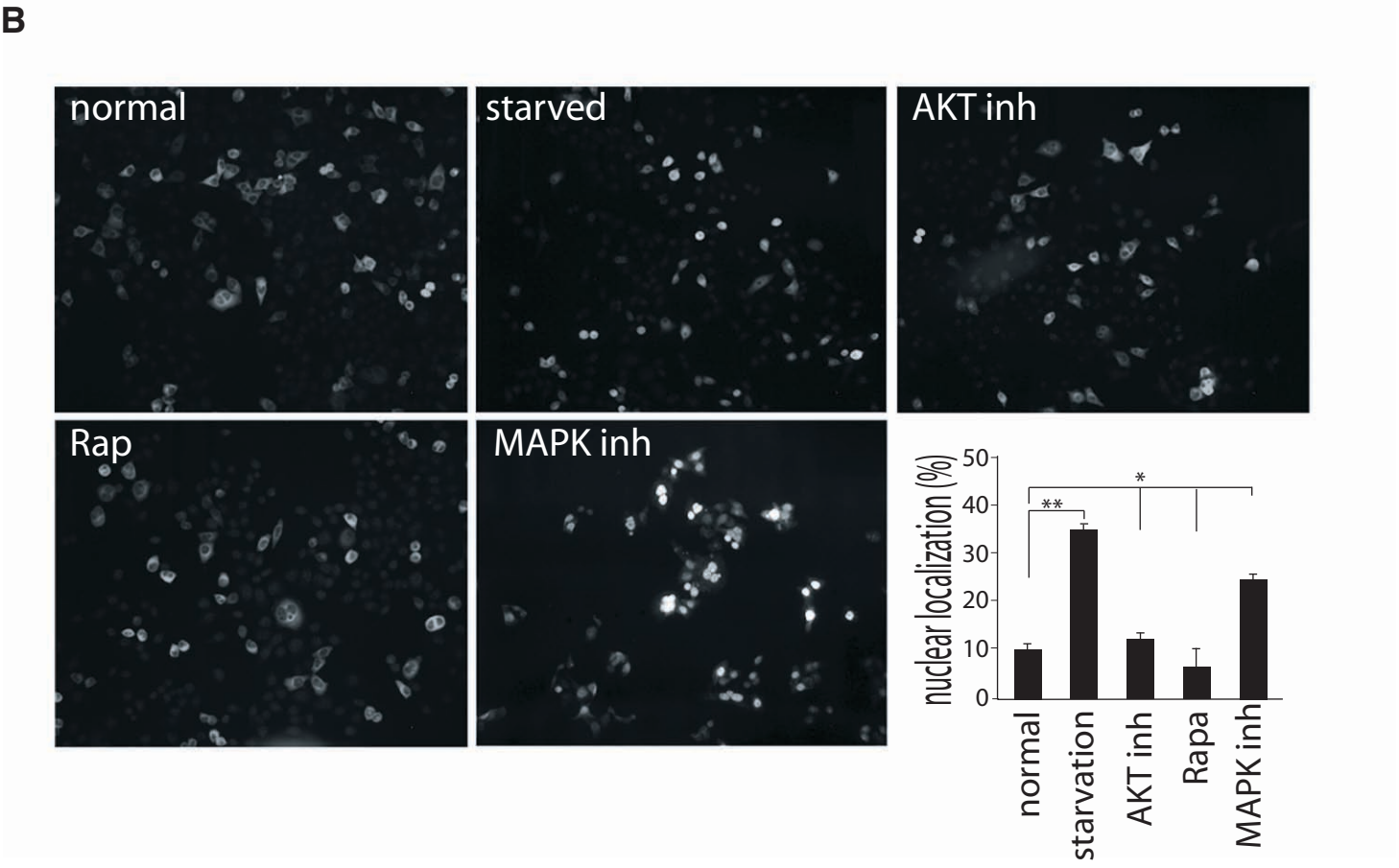

Supplementary Fig. 9 Starvation induces TFEB nuclear translocation through MAPK. (A) Starvation induces cytosolic TFEB mobility shift and nuclear translocation. Normal medium; starved medium (4h); starved + normal, indicates that cells were cultured in starved medium (4h) and supplemented with normal medium 1h prior to harvesting. Cytosolic and nuclear fractions were subjected to Flag immunoblotting. (B) Analysis of TFEB cellular localization by immunofluorence in HeLa cells treated as indicated in Fig. 2G. The graph shows percentage of cells that display TFEB nuclear localization. Experiments were performed in triplicate. Error bars represent standard deviations; p value (*)< 0.05; (**)< 0.01.

Supplementary Fig. 10

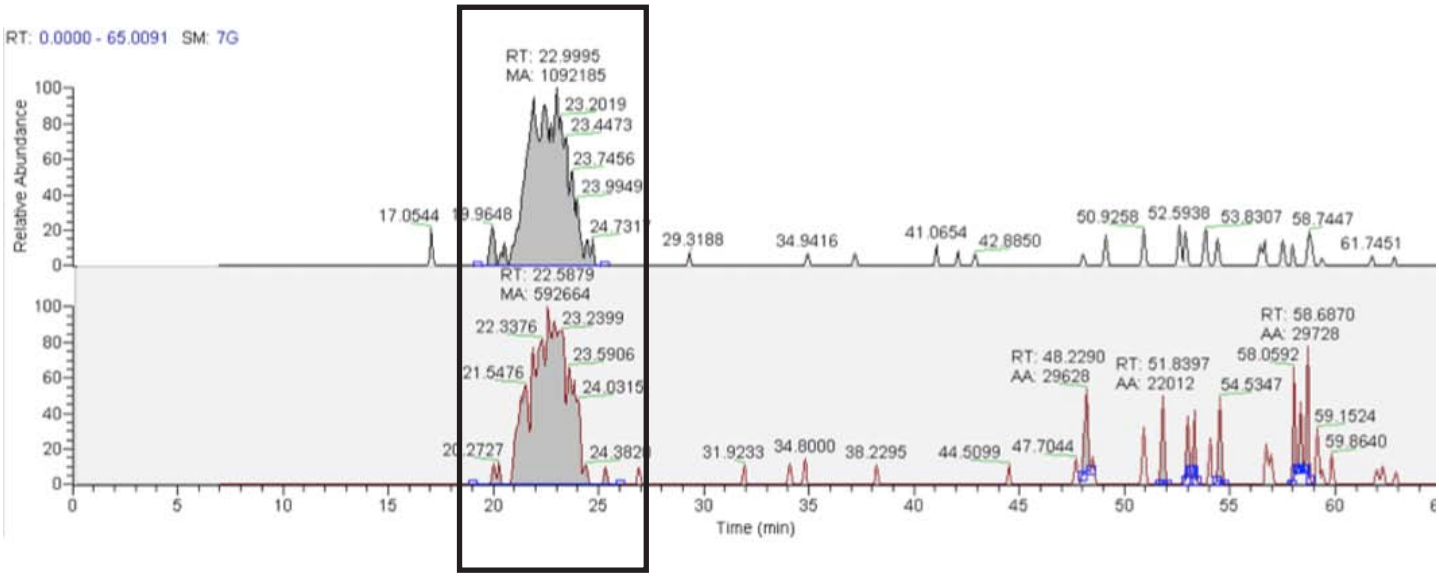

Supplementary Fig. 10 TFEB is dephosphorylated during starvation. The HPLC elution profile of phosphorylated peptide containing serine 142 eluted from control (upper panel) and starved samples (lower panel) was obtained from LTQ-Velos-orbitrap. The area under the curve (AUC) indirectly reflects relative peptide amount in the two samples. Based on the AUC the degree of peptide phosphorylation in the control sample is approximately 2 fold higher than in the starved sample. Here we show a representative image of 5 independent experiments.

Supplementary Fig. 11

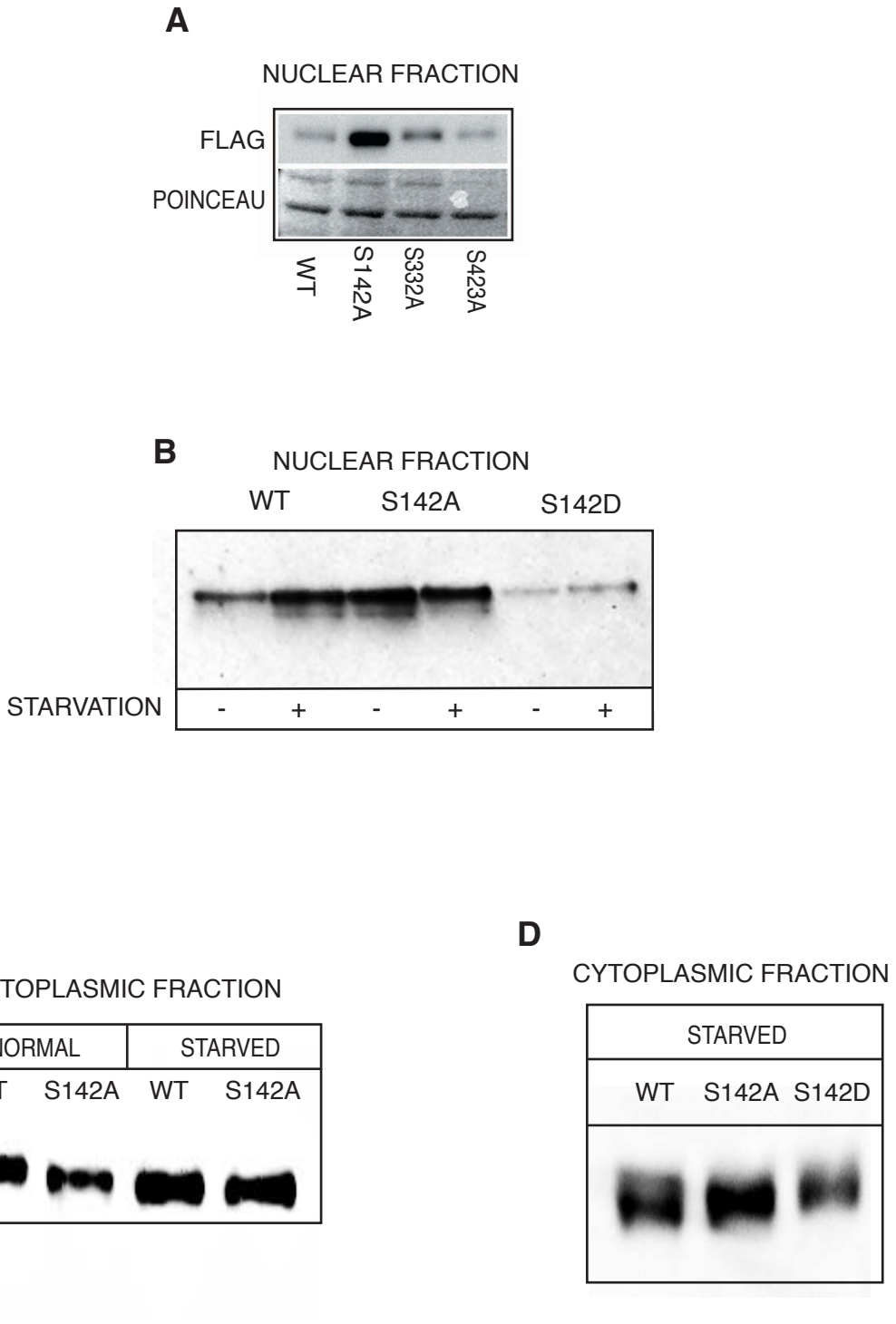

Supplementary Fig. 11 TFEB nuclear traslocation is dependent on S142 phosporylation. (A) HeLa cells expressing TFEB WT-, S142A-, S332A- or S423A-3xFlag proteins were subjected to nuclear protein isolation. Equal amounts of nuclear proteins were verified by poinceau staining. (B) HeLa cells expressing TFEB WT-, S142A- and S142D-3xFlag proteins were subjected to nuclear protein isolation in normal and starved conditions. (C) Flag immunoblotting of cytosolic protein isolated from HeLa cells expressing TFEB WT- and TFEB-S142A-3xFlag shows that in normal media S142A migrates as lower MW band compared to WT TFEB as opposed to starved conditions where this shift is not evident. (D) Flag immunoblotting of cytosolic protein isolated from starved HeLa cells expressing TFEB WT-, S142A- and S142D-3xFlag shows a reduced shift of TFEB-S142D. All the experiments were performed in triplicate.

Supplementary Fig. 12

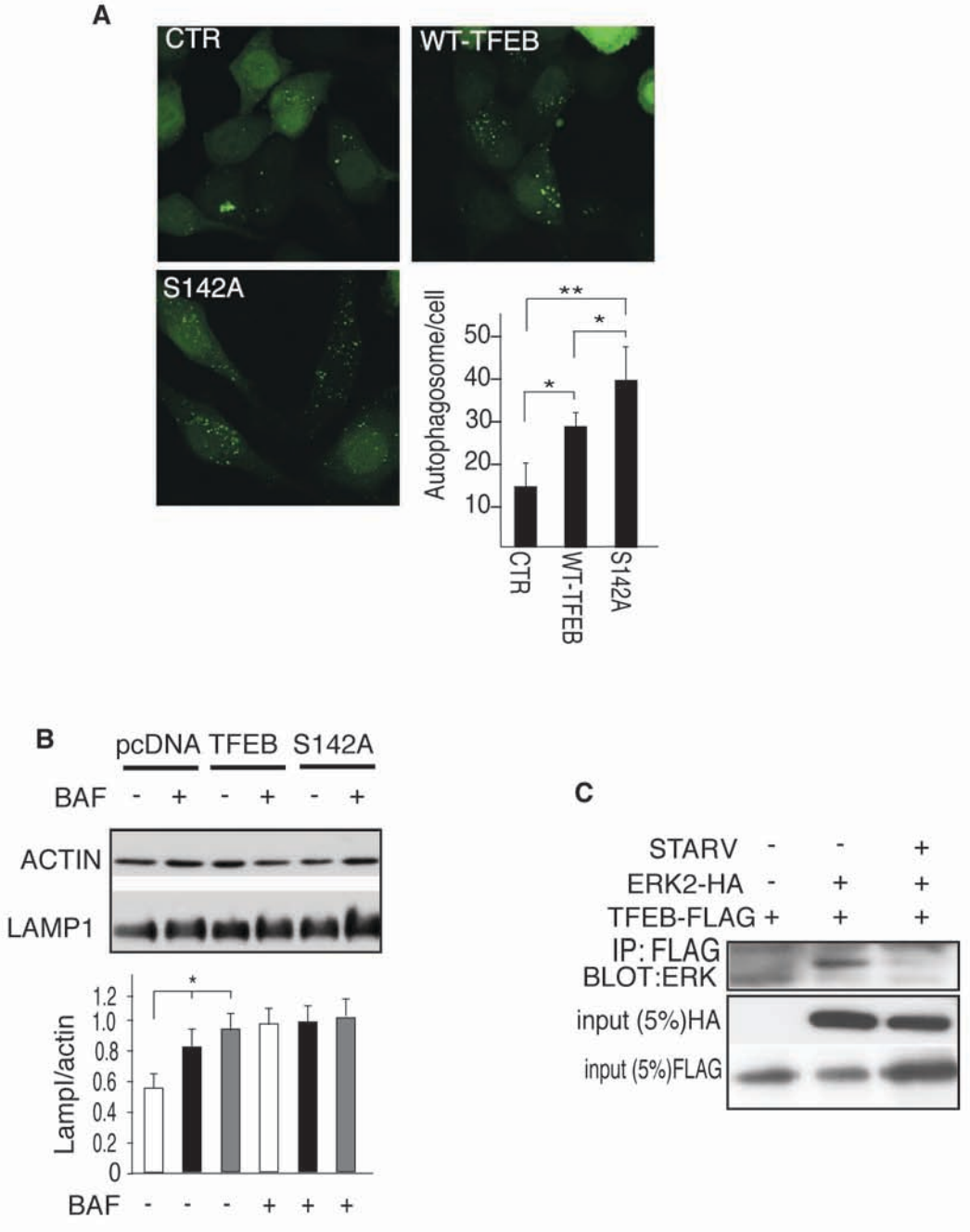

Supplementary Fig. 12 S142A TFEB mutant displays enhanced activity. (A) HeLa cells stably over-expressing GFP-LC3 were transfected with equal amounts of empty, TFEB WT- or TFEB S142A-3xFlag plasmids and the number of autophagosomes was quantified. At least ten fields (containing 4-10 cells) were analyzed for each point. (B) Western blot analysis of Lamp1 in protein extracts from HeLa cells transfected with equal amounts of empty (pcDNA), TFEB WT- or TFEB S142A-3xFlag vectors. Bafilomycin was added where indicated (4h 400nM). Quantification of protein levels was normalized to actin levels. (C) Western blot analysis using anti-Erk antibody on HeLa cells transfected with HAErk2 and/or TFEB-3xFlag, kept in full serum or nutrient starved for 4h and immunoprecipitated with anti-Flag antibody. Lysates were immunoprecipitated with anti-FLAG and blotted with an anti-Erk antibody. Experiments were performed in triplicate. Error bars represent standard deviations; p value (*)< 0.05; (**)< 0.01.

Supplementary Fig. 13

Supplementary Fig. 13 Multiple sequence alignment of TFEB-human S142 phosphorylation site with TFEB paralogues, MITF and relevant TFEB-related family members. TFEB_human homologs were identified by BLAST (2.2.17) search against UniProtKB database at ExPASy Proteomics Server. We removed the hits with “putative”, “uncharacterized” and “cDNA” keywords and hits without gene names. Next, we aligned the remaining homologs with ClustalW (1.82). The multiple sequence alignment was generated by Seaview. The figure shows only a 20 amino acid-long segment of TFEB_HUMAN sequence aligned with other proteins from TFEB, MITF, TCFEB, TFE3 and TCFE3 families. “sp” stands for SwissProt entry, while “tr” denotes Tremble entry. P19484 is a UniProrKB accession code. TFEB_HUMAN indicates gene name and species name respectively.

Supplementary Fig. 14

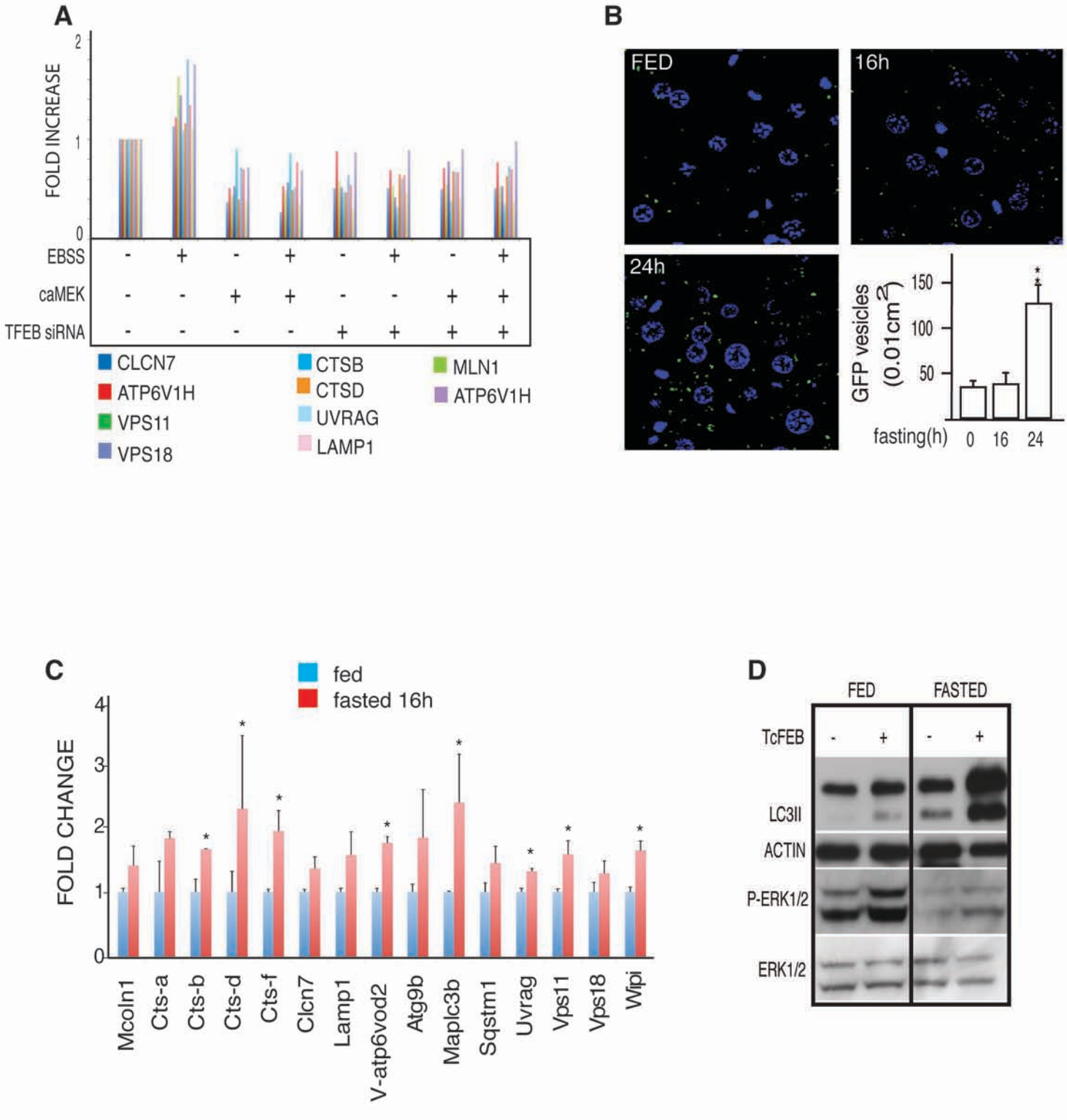

Supplementary Fig. 14 In vivo analysis of TFEB-mediated induction of autophagy.
(A) qPCR analysis of lysosomal and autophagic TFEB-target genes in TFEB siRNA or TFEB-scrambled control cells transfected with either a constitutive active MEK (caMEK) plasmid or with an empty vector. Starvation was performed where indicated. (B) Immunofluorescence analysis of GFP-positive vesicles in fed, 16h- and 24h-fasted mice. Quantification of vesicles is shown in the graph. (C) qPCR analysis of TFEB target gene expression in liver samples from fed and fasted animals (n=3/group). Gapdh and Hprt were used as reference genes. (D) Western blot analysis of LC3, actin, p-ERK1/2 and ERK1/2 in liver extracts from mice injected with AAV2/9 Tcfeb-HA. Error bars represent standard deviations; p value (*)<0.05; (**)<0.01.

Supplementary Fig. 15

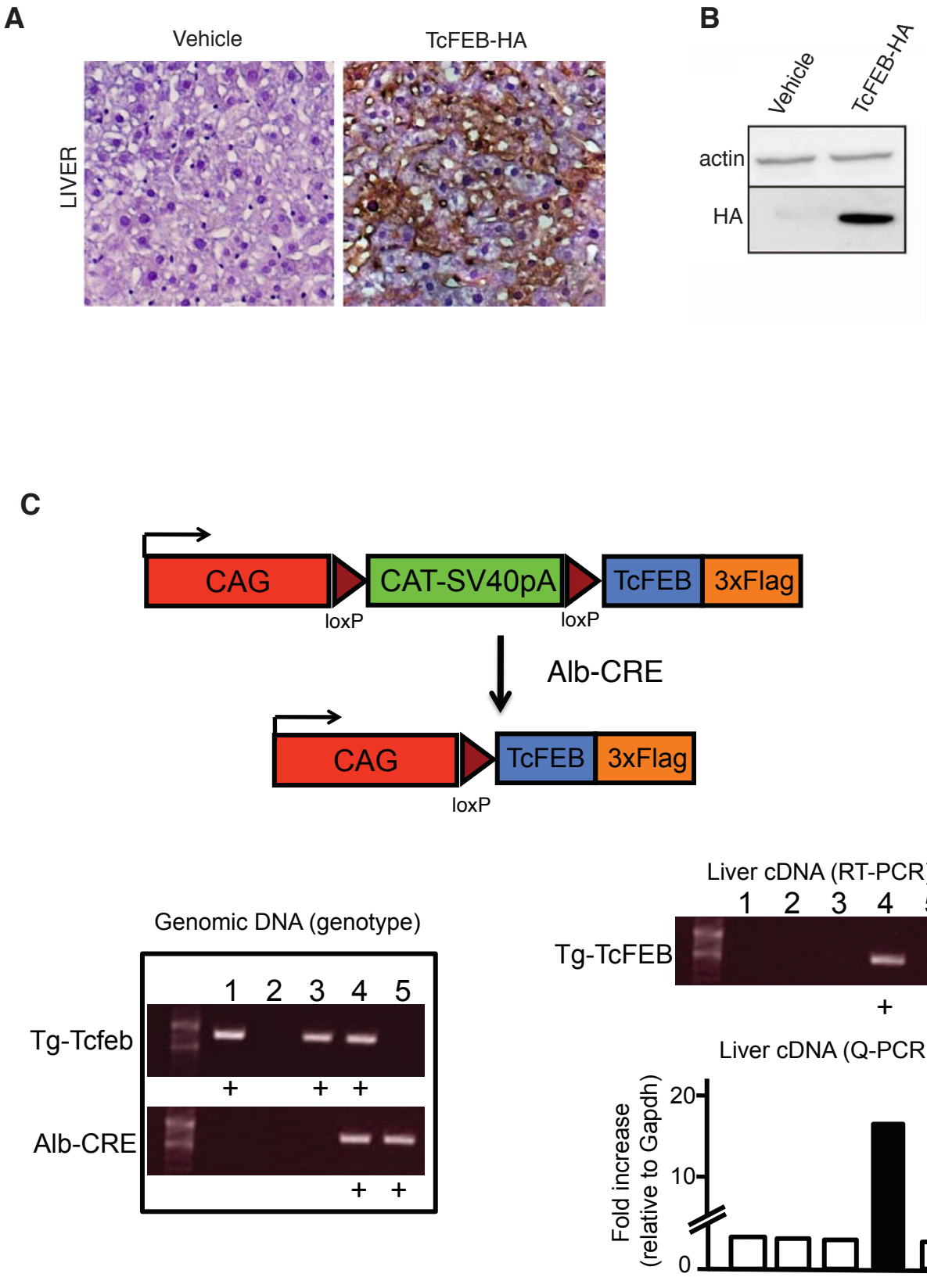

Supplementary Fig. 15 Strategy for TcFEB overexpression in vivo. (A) Representative images of cryo-preserved liver slices immunostained with anti-HA antibody (to verify viral transduction efficiency). (B) Liver protein extracted from TcFEB-HA injected and control mice were immunoblotted HA and actin antibodies. (C) Generation of a transgenic mouse line for TcFEB conditional overexpression. The map of the transgene vector, before and after CRE recombinase is illustrated at the top. Representative genotypes of littermates are shown on the left, while the correspondent liver-specific TcFEB overexpression in mouse n4 is shown on the right (RT PCR was performed with flag specific oligos, while qPCR with TcFEB specific oligos).

Supplementary Table 1: Gene expression changes in response to TFEB overexpression or cell starvation

PEARSON CORRELATION 0.42

TFEB stable OVEREXPRESSION	
GENE SYMBOL	FOLD INCREASE
AKT1	1.2
AMBRA1	1.2
APP	1.4
ARSA	1.3
ATG10	1.1
ATG12	1.2
ATG16L1	-1.2
ATG16L2	1.1
ATG3	1.2
ATG4A	1.2
ATG4B	1.3
ATG4C	1.1
ATG4D	1.6
ATG5	1.2
ATG7	1.2
ATG9A	1.1
ATG9B	5.6
BAD	1.0
BAK1	1.4
BAX	1.2
BCL2	1.5
BECN1	1.2
BID	1.2
BNIP3	1.1
CLN3	1.5
CXCR4	1.3
DRAM	1.8
EIF2AK3	1.4
EIF4G1	1.3
FAM176A	1.6
GAA	1.3
GABARAP	1.1
GABARAPL1	1.0
GABARAPL2	1.1
HGS	-1.1
HTT	1.0
MAP1LC3A	1.1
MAP1LC3B	1.2
PIK3C3	-1.2
PIK3R4	1.1
PTEN	1.1
RAB24	1.2
RGS19	1.2
SNCA	1.6
SQSTM1	2.4
TP53	1.1
ULK1	1.1
UVRAG	1.8
VPS11	1.4
VPS18	1.4
WIPI	2.5

CELL STARVATION	
GENE SYMBOL	FOLD INCREASE
AKT1	1.1
AMBRA1	1.3
APP	1.2
ARSA	1.4
ATG10	1.0
ATG12	1.2
ATG16L1	-1.5
ATG16L2	1.0
ATG3	1.0
ATG4A	-1.2
ATG4B	1.1
ATG4C	1.1
ATG4D	1.8
ATG5	1.1
ATG7	1.0
ATG9A	1.3
ATG9B	1.8
BAD	1.0
BAK1	1.0
BAX	1.1
BCL2	1.4
BECN1	1.0
BID	1.1
BNIP3	1.1
CLN3	1.2
CXCR4	1.2
DRAM	-1.3
EIF2AK3	1.2
EIF4G1	-1.2
FAM176A	-1.3
GAA	1.2
GABARAP	1.3
GABARAPL1	1.2
GABARAPL2	1.0
HGS	-1.2
HTT	1.0
MAP1LC3A	1.4
MAP1LC3B	1.2
PIK3C3	-1.2
PIK3R4	-1.2
PTEN	1.1
RAB24	1.2
RGS19	-1.2
SNCA	-1.2
SQSTM1	1.6
TP53	1.0
ULK1	2.0
UVRAG	2.4
VPS11	1.6
VPS18	1.4
WIPI	1.5

Pearson product-moment correlation coefficient (PMCC) was obtained by comparing the gene expression profiles shown, i.e. TFEB stable overexpression vs. gene expression profiles of starved HeLa cells.

Supplementary Table 2: Expression changes in autophagy genes in response to TFEB overexpression

TFEB stable OVEREXPRESSION			TFEB Transient OVEREXPRESSION		TET-ON TFEB OVEREXPRESSION	
GENE SYMBOL	FOLD INCREASE		GENE SYMBOL	FOLD INCREASE	GENE SYMBOL	FOLD INCREASE
AKT1	1.25		AKT1	1.10	AKT1	1.09
AMBRA1	1.18		AMBRA1	-1.30	AMBRA1	1.03
APP	1.44		APP	1.03	APP	1.03
ARSA	1.25		ARSA	1.19	ARSA	1.06
ATG10	1.07		ATG10	-1.26	ATG10	1.52
ATG12	1.16		ATG12	1.00	ATG12	1.10
ATG16L1	-1.20		ATG16L1	-1.37	ATG16L1	1.00
ATG16L2	1.15		ATG16L2	-1.79	ATG16L2	-1.45
ATG3	1.20		ATG3	1.01	ATG3	1.21
ATG4A	1.23		ATG4A	1.35	ATG4A	1.27
ATG4B	1.26		ATG4B	1.13	ATG4B	1.09
ATG4C	1.07		ATG4C	1.20	ATG4C	1.24
ATG4D	1.59	*	ATG4D	1.16	ATG4D	1.43
ATG5	1.21		ATG5	1.10	ATG5	1.37
ATG7	1.25		ATG7	1.09	ATG7	1.07
ATG9A	1.09		ATG9A	-1.31	ATG9A	-1.22
ATG9B	5.62	*	ATG9B	7.87	ATG9B	2.51
BAD	1.04		BAD	1.08	BAD	1.09
BAK1	1.37		BAK1	1.05	BAK1	1.13
BAX	1.15		BAX	1.11	BAX	1.13
BCL2	1.51	*	BCL2	1.78	BCL2	2.51
BECN1	1.17		BECN1	1.16	BECN1	1.06
BID	1.16		BID	1.01	BID	1.19
BNIP3	1.08		BNIP3	1.20	BNIP3	1.04
CLN3	1.47	*	CLN3	1.45	CLN3	1.41
CXCR4	1.33		CXCR4	1.09	CXCR4	1.14
DRAM	1.78		DRAM	1.00	DRAM	1.04
EIF2AK3	1.43		EIF2AK3	1.06	EIF2AK3	1.27
EIF4G1	1.27		EIF4G1	1.11	EIF4G1	-1.34
FAM176A	1.63		FAM176A	1.07	FAM176A	1.12
GAA	1.33		GAA	1.01	GAA	1.08
GABARAP	1.07		GABARAP	1.14	GABARAP	1.14
GABARAPL1	1.01		GABARAPL1	1.13	GABARAPL1	-1.23
GABARAPL2	1.05		GABARAPL2	-1.68	GABARAPL2	1.08
HGS	-1.06		HGS	-1.16	HGS	1.05
HTT	1.01		HTT	1.08	HTT	1.51
MAP1LC3A	1.15		MAP1LC3A	1.10	MAP1LC3A	1.13
MAP1LC3B	1.25	*	MAP1LC3B	1.97	MAP1LC3B	1.46
PIK3C3	-1.23		PIK3C3	-1.18	PIK3C3	1.02
PIK3R4	1.08		PIK3R4	1.10	PIK3R4	-1.20
PTEN	1.06		PTEN	1.10	PTEN	1.06
RAB24	1.15		RAB24	1.10	RAB24	1.11
RGS19	1.22		RGS19	1.11	RGS19	1.13
SNCA	1.57	*	SNCA	1.32	SNCA	1.38
SQSTM1	2.42	*	SQSTM1	1.36	SQSTM1	1.82
TP53	1.08		TP53	1.18	TP53	1.06
ULK1	1.06		ULK1	-1.27	ULK1	-1.28
UVRAG	1.75	*	UVRAG	2.16	UVRAG	1.48
VPS11	1.39	*	VPS11	1.80	VPS11	1.51
VPS18	1.38	*	VPS18	3.22	VPS18	2.01
WIPI	2.48	*	WIPI	2.86	WIPI	1.98

51 genes with a reported involvement in autophagy were tested using several conditions of TFEB overexpression (stable, transient and tetracycline inducible). Fold increase represents the average of 4 independent experiments. Genes whose expression is significantly up-regulated are indicated in red ($p < 0.05$).

Supplementary Table 3: Gene expression changes in response to TFEB inhibition using siRNA

GENE SYMBOL	FOLD INCREASE
AKT1	-2.1962
AMBRA1	1.1134
APP	-1.1769
ARSA	-2.858
ATG10	1.0389
ATG12	1.0461
ATG16L1	-1.6529
ATG16L2	-1.3333
ATG3	1.2702
ATG4A	-1.3333
ATG4B	-1.244
ATG4C	-1.6077
ATG4D	-1.1527
ATG5	-1.0607
ATG7	-1.6994
ATG9A	-1.9793
ATG9B	-4.4229
BAK1	1.4489
BAX	-1.3803
BCL2	-2.3054
BECN1	-1.1769
BID	1.3241
BNIP3	-1.1212
CLN3	-1.4692
CXCR4	-1.5529
DRAM	-1.1769
EIF2AK3	-1.3996
EIF4G1	-2.3702
ESR1	-1.676
GAA	-1.3613
GABARAP	1.4093
GABARAPL1	-1.2016
GABARAPL2	1.3899
HGS	-1.5594
HTT	-1.3899
MAP1LC3A	-1.0389
MAP1LC3B	-1.4175
PIK3R4	-1.6189
PTEN	-1.2702
RAB24	1.3333
SNCA	1.2269
SQSTM1	-1.4093
TP53	-1.279
ULK1	-3.668
UVRAG	-1.3059
VPS11	-1.84
VPS18	-2.1
WIPI	-1.94

Down-regulated genes upon siRNA-mediated TFEB knock-down. Fold change represents the average of 4 independent experiments. Genes significantly down-regulated are indicated in red ($p < 0.05$).

Supplementary Table 4: Prediction of protein kinases for S142 phosphorylation using different bioinformatics methods

METHODS	Confidence Score Cutoff	Actual prediction for S142	Group	Family	Subfamily	Kinase
CrPhos0.8	FPR ≤ 30%	MAPK8	CMGC	MAPK	JNK	MAPK8
CrPhos0.8	FPR ≤ 30%	MAPK3	CMGC	MAPK	ERK	MAPK3
CrPhos0.8	FPR ≤ 30%	MAPK1	CMGC	MAPK	ERK	MAPK1
CrPhos0.8	FPR ≤ 30%	CDK2	CMGC	CDK	CDK2	CDK2
GPS-2.1	Score ≥ 5	CMGC/CDK/CDK5	CMGC	CDK	CDK5	
GPS-2.1	Score ≥ 5	CMGC/CDK/CDK4/CDK4	CMGC	CDK	CDK4	CDK4
GPS-2.1	Score ≥ 5	CMGC/MAPK/ERK/MAPK1	CMGC	MAPK	ERK	MAPK1
GPS-2.1	Score ≥ 5	CMGC/MAPK/ERK/MAPK3	CMGC	MAPK	ERK	MAPK3
GPS-2.1	Score ≥ 5	CMGC/MAPK/JNK/MAPK8	CMGC	MAPK	JNK	MAPK8
GPS-2.1	Score ≥ 5	CMGC/MAPK/JNK/MAPK10	CMGC	MAPK	JNK	MAPK10
GPS-2.1	Score ≥ 5	STE/STE7/MAP2K7	STE	STE7	MAP2K7	
GPS-2.1	Score ≥ 5	CMGC/MAPK/p38/MAPK12	CMGC	MAPK	p38	MAPK12
PhosphoMotifFinder		GSK3	CMGC	GSK	GSK3	
PhosphoMotifFinder		ERK1	CMGC	MAPK	ERK	MAPK3
PhosphoMotifFinder		ERK2	CMGC	MAPK	ERK	MAPK1
PhosphoMotifFinder		ERK3	CMGC	MAPK	ERK	MAPK6
PhosphoMotifFinder		CDK5	CMGC	CDK	CDK5	CDK5
networkin		p38MAPK/MAPK9	CMGC	MAPK	JNK	MAPK9
networkin		GSK3/GSK3B	CMGC	GSK	GSK3	GSK3B
networkin		CDK5/CDK2	CMGC	CDK	CDK2	CDK2
networkin 2		CDK2_CDK3/CDK2	CMGC	CDK	CDK2	CDK2
PHOSIDA		CK1_group	CK1	CK1		
PHOSIDA		ERK	CMGC	MAPK	ERK	

The list of putative protein kinases for phosphorylation of S142 predicted by different bioinformatics methods. The names are listed in the first column. The entries in the second column show prediction confidence score cutoff used to select reliable predictions, if available. For example, four predictions from CrPhos0.8 with false positive rate (FPR) less than 30% are listed in the table. GPS-2.1's confidence score is calculated as the distance between the score and threshold assigned for a particular prediction. The cutoff entries for the methods with no explicit confidence scores are left blank. All predictions made by such methods are selected. The third column includes the predictions of the methods as given in their actual output format. The next four columns show the classification of actual predictions in terms of kinase group, kinase family, kinase subfamily and protein kinase to describe predictions in a standard format as obtained from KinBase database (http://kinase.com/kinbase/).

Supplementary table 5: in vitro kinase assay raw data

Kinases tested

Kinase	Batch No.	Concentration (mg/mL)	Concentration (ng/well)
AMPKα1(h)	D8HN073N	0.96	2
AMPKα2(h)	D8SN007N	1.92	9.6
P70S6K(h)	611044302	3.53	17.6
PKBβ(h)	D7JN061U	3.72	46.5
PKBγ(h)	25712U	3.92	0.33
mTOR(h)	D8CN062U	0.29	72.5
GSK3α(h)	25830U	1.12	9.4
GSK3β(h)	25744U	3.03	12.6
MAPK1(h)	D7NN031U	3.13	13.1
MAPK2(h)	33015U	1.14	47.3
Rsk1(h)	1631899	0.7	4.4
Rsk2(h)	31101U	1.65	2.1
Rsk3(h)	LB250LMp66	2	25
PKBα(h)	D8MN034U	1.83	45.8

Mean Cpms					Acid Blanks		
	Ctrl Peptide	TFEB-A142	TFEB-S142	No Peptide	Ctrl Peptide	TFEB-A142	TFEB-S142
AMPKα1(h)	1569	185	205	447	249	287	303
AMPKα2(h)	2962	166	257	519	265	243	324
p70S6K(h)	688	96	175	1121	145	217	290
PKBβ(h)	3501	126	275	355	213	253	335
PKBγ(h)	3803	77	209	153	234	256	238
mTOR(h)	8985	372	513	487	265	174	207
GSK3α(h)	5438	456	458	325	333	329	358
GSK3β(h)	5208	421	482	2192	342	451	400
MAPK1(h)	12122	540	2097	386	265	229	323
MAPK2(h)	8919	395	909	347	243	229	234
Rsk1(h)	9894	329	300	469	223	183	187
Rsk2(h)	7193	268	223	323	277	288	270
Rsk3(h)	9641	450	453	323	301	310	354
PKBα(h)	6134	405	334	243	333	373	341

Standard Deviation					Acid Blanks		
	Ctrl Peptide	TFEB-A-142	TFEB-S-142	No Peptide	Ctrl Peptide	TFEB-A-142	TFEB-S-142
AMPKα1(h)	288	69	29	355	66	42	34
AMPKα2(h)	344	4	55	310	80	7	11
p70S6K(h)	4	8	64	854	91	2	17
PKBβ(h)	59	13	54	98	41	51	33
PKBγ(h)	346	21	23	30	25	29	11
mTOR(h)	436	81	47	24	47	29	66
GSK3α(h)	137	49	76	37	8	19	11
GSK3β(h)	6	48	41	2628	87	21	54
MAPK1(h)	261	76	228	240	40	14	14
MAPK2(h)	227	8	33	214	63	24	11
Rsk1(h)	738	78	23	515	74	5	8
Rsk2(h)	885	28	32	184	45	21	64
Rsk3(h)	1327	20	62	24	62	30	4
PKBα(h)	204	106	112	16	45	72	1

The data shown in the results section suggests that MAPK1 (ERK2) and to a lesser extent MAPK2 (ERK1) are capable to phosporylate TFEB-S-142. There is a clear distinction between TFEB-A-142 and TFEB-S-142, likely due to the alanine substitution in the sequence of TFEB-A-142. Other serines within this sequence do not appear to become phosphorylated under our assay conditions, or are only weakly phosphorylated, remaining below our limit of detection. All protein kinases were used at their standard KinaseProfiler™ assay concentration (MILLIPORE)